

Multi-channel, tunable quantum photonic devices on fiber-integrated platforms

Woong Bae Jeon¹, Jong Sung Moon^{1,2}, Kyu-Young Kim¹, Mohamed Benyoucef³, and Je-Hyung Kim^{1,}*

¹Department of Physics, Ulsan National Institute of Science and Technology (UNIST), Ulsan 44919, Republic of Korea

²Quantum Technology Research Division, Electronics and Telecommunications Research Institute (ETRI), Daejeon, 34129, Republic of Korea

³Institute of Physics, INA, University of Kassel, Heinrich-Plett-Str. 40, Kassel, 34132, Germany

*jehyungkim@unist.ac.kr,

KEYWORDS

Quantum dots, Single-photon sources, Fiber-integrated quantum devices, Scalable quantum photonics,

ABSTRACT

Scalable, reliable quantum light sources are essential for increasing quantum channel capacity and advancing quantum protocols based on photonic qubits. Although recent developments in solid-state quantum emitters have enabled the generation of single photons with high performance, the scalable integration of quantum devices onto practical optical platforms remains a challenging task. Here, we present a breakthrough in achieving a multiple, tunable array of quantum photonic devices. The selective integration of multiple quantum dot devices onto a V-groove fiber platform features scalability, tunability, high yield, and high single-photon coupling efficiency. Therefore, our fiber-integrated quantum platform realizes a scalable and reliable single-photon array within a compact fiber chip at telecom wavelengths.

Recent advances in solid-state quantum emitters have enabled the efficient generation of single and entangled photons with high purity, indistinguishability, and fidelity.¹⁻³ For practical and reliable utilization of these quantum photonic resources, the heterogeneous integration of quantum emitters with low-loss optical fibers⁴ is essential in future quantum applications across optical fiber networks. So far, fiber-integrated quantum emitters have been realized through several approaches, including a lensed fiber,⁵ micro-optics,⁶ and adiabatic coupling.^{7, 8} More practical plug-and-play type single-photon sources have been demonstrated by directly gluing a fiber on a quantum dot (QD) wafer⁹⁻¹¹ and also directly integrating a single QD device onto a fiber.^{12, 13}

While such fiber-coupled single-photon sources would be useful for a simple quantum key distribution scheme,¹⁴ the most advanced photonic quantum applications, such as quantum neural networks¹⁵ and quantum simulators,^{16, 17} require multi-channel quantum light sources. Multiple single-photon sources are also useful for creating large-scale quantum entanglement, such as high-dimensional photonic graph states.¹⁸ A spatial demultiplexing technique with temporally separated photons from a single QD has been introduced to realize a multiple array of single photons and has demonstrated multi-photon boson sampling.¹⁶ Whereas the demultiplexing method efficiently generates indistinguishable multiple single photons from a single emitter, it sacrifices the generation rate with increasing channels. Alternatively, generating single photons from individual quantum emitters at each channel provides more versatile multiple single-photon arrays. In previous approaches, periodically patterned QD devices on a chip have been coupled with multi-channel fibers via precise alignment⁹ or photonic wiring.¹⁹ However, this chip-to-fiber integration lacks the efficiency, selectivity, and tunability of the coupled quantum emitters. In particular, solid-state quantum emitters suffer from large randomness in their positions and frequencies. Therefore, this simple fiber array of single-photon sources has a low yield of the integrated devices, and each

channel generates single photons with random frequency, which poses significant limitations to being deployable sources for quantum applications.

Here, we demonstrate multi-channel and tunable single-photon sources on fiber-integrated platforms. We address previous challenges by developing a multi-functional fiber platform that integrates multiple QD devices, efficiently couple single photons through a fiber array, and apply electric field for spectral tuning. Our integration, interfacing, and engineering techniques enable selective integration of emitters at desired wavelengths, efficient coupling of single photons, and fine frequency tuning in a fiber-integrated chip.

Scalable integration of multiple quantum emitters was conducted by transferring telecom-emitting InAs/InP QD devices⁶ onto optical fibers. The QD sample used was grown by molecular beam epitaxy on an InP substrate^{20, 21}. A 1400 nm InGaAs sacrificial layer was initially deposited to fabricate air-suspended cavities. This was followed by the growth of a 150 nm thick InP layer, subsequent growth of InAs QDS, and finally, a 150 nm thick InP capping layer is grown. In order to realize fiber-integrated single-photon arrays, we first developed a multi-functional fiber-integrated platform. Figure 1(a) describes a schematic image of QD devices integrated on a multi-channel V-groove fiber array. QDs require cryogenic temperature to generate single photons with high purity and indistinguishability, whereas the integrated fibers lack thermal conductivity. To resolve this cooling issue in the fiber-integrated quantum devices, we coated the front surface of a V-groove silicon fiber block, including a standard SMF-28 fiber array, with a 50 nm thick gold film. Then, we etched the metal film at fiber cores to a depth of over 70 nm using a focused ion beam. Our QD membrane devices are designed to be slightly larger than the etched metal hole. Therefore, the deposited gold film effectively cools down the QD device, and the etched metal at the fiber core serves as an optical window for single-photon transmission from the

integrated QDs. Then, the metal-coated Si fiber block was mounted on the metal mold connected to the cryostat. Therefore, the fiber-integrated QDs are thermally connected through a coated metal thin film, a Si block, and a cold finger of the cryostat and can be cooled for low-temperature operation (10 K). In addition, to apply electrical bias, we grounded the deposited gold film on a fiber facet and placed another electrode at a distance. Therefore, two electrodes apply an electric field to the QDs for spectral tuning.

Coupling single photons from QDs into a single-mode fiber demands optimal optical interfaces to enhance light extraction and mode-matching conditions. A thin-membrane structure with proper cavity design provides a suitable interface for stable device-to-fiber integration. For example, a well-known ring-based circular Bragg gratings structure^{22, 23} could provide a vertical Gaussian beam. However, its small mode size due to its large refractive index still limits the coupling efficiency of a fiber. Introducing a hybrid structure could enhance the coupling efficiency, but it requires a complicated reflector design.²⁴ Recently, we have developed hole-based circular Bragg grating (hole-CBG), which enables a narrow Gaussian beam that matches the single-mode fiber.¹³ Compared to conventional ring structures, such a hole-based design has shown better performance as diffraction optics with suppressed high-order diffraction, leading to a much tighter focusing spot in a lens^{25, 26} and vertically directional emission in a cavity.¹³ Etched holes arranged azimuthally on a subwavelength scale form reduced effective refractive index.²⁷ This spreads out a spatial cavity mode more widely, as shown in Figure 1(c), leading to a reduction in the divergence in momentum space according to the Fourier transform relationship. We optimized the hole diameter and axial and radial distance between holes to achieve 60 percent of far-field emission within 7 degrees (Figure 1(d)). As shown in Figure 1(b), from the simulation of a fiber-integrated hole-CBG device, including a partial reflection by the top electrode, we

calculate a fiber coupling efficiency of 58.5% for an optimized electrode distance of about 800 nm. Together with the optimized far-field emission, we calculated a Purcell factor of 120 at a cavity mode having a calculated quality factor of 4,000.

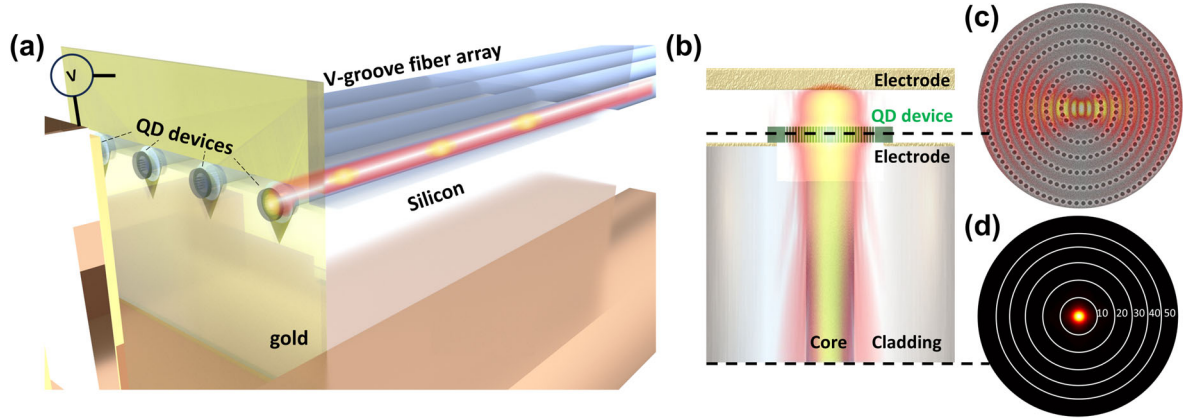


Figure 1. (a) Schematic image of a multi-channel, tunable single-photon arrays based on a fiber-integrated platform. (b) Detailed configuration of a fiber-integrated QD device with metal layers for low-temperature cooling and applying electric field. A cross-sectional electric field profile is displayed in log scale. (c) SEM image of a fabricated InAs/InP QD cavity with a superimposed near-field cavity mode profile. (d) Calculated far field mode profile of the dipole-coupled cavity.

Figure 2(a) shows the array of fabricated hole-CBG devices on an InAs/InP QD sample during the transfer process. We transfer individual hole-CBG devices via a polydimethylsiloxane (PDMS) microstamp under an optical microscope. The microstamp has a radius of 20 μm and a height of 7 μm for picking up a single hole-CBG device. We brought the cylindrical microstamp closer to each device, picked them up, and integrated them on each channel of the V-groove optical fiber array. Figure 2(b) shows microscope images of a gold-coated V-groove fiber array with an etched fiber core. Figure 2(c) shows that QD devices are firmly integrated on a V-groove fiber array by Van der Waals force.

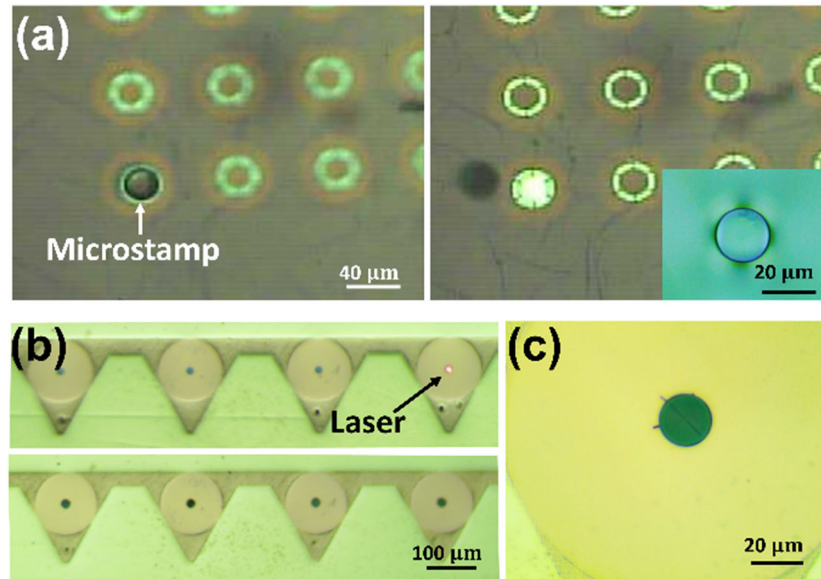


Figure 2. (a) Optical microscopy images captured during transfer of a QD device using a PDMS microstamp. The left (right) image shows the microstamp approaching (picking up) the QD device. Inset shows the magnified PDMS microstamp. (b) Microscopy images of a gold-coated V-groove fiber array before (top) and after (bottom) the transfer of QD devices. A 633 nm red laser passing through the etched fiber cores is clearly visible in the top image. The bottom image shows four QD devices integrated onto each fiber channel. (c) A closer view of the fiber-integrated QD device.

We optically characterize single-photon emission from the fiber-integrated QD devices at a low temperature of 10 K. Figure 3(a) describes an all-fiber connectorized single-photon system from a laser to a single QD and single-photon detectors. A fiber-coupled 785 nm laser was sent to the fiber-quantum channel by a 10:90 beamsplitter and excited the QD device. The photoluminescence (PL) signal from the QDs was coupled to a fiber and transmitted to a high-resolution spectrometer for spectrum measurements or a fiber-based spectral filter followed by a fiber-based Hanbury Brown and Twiss interferometer for photon-correlation measurement. Therefore, our system operates on an all-fiber basis without any optical alignment. Figure 3(b) displays an optical image of the multi-channel single-photon array mounted on a cryostat. Electrical signals were also connected to our fiber platform to induce voltage.

Figure 3(c) shows the PL spectrum from the fiber-integrated QD device. The single QD at 1228 nm shows a highly enhanced signal near the cavity mode. The photon correlation data of spectrally filtered single QD emission clearly show an antibunching nature in the inset of Figure 3(c). Nonzero $g^{(2)}(0) = 0.2$ mostly originates from spectrally superimposed broad background cavity emission due to high density QD emission. From the separately measured system efficiency of 35.6%, including the transmission losses in fiber connectors and spectral filter, and the detection efficiency of single-photon detectors, we calculated the single-photon coupling efficiency of 9% at the end of the first fiber. Multi-photon events by nonzero $g^{(2)}(0)$ was also corrected for calculating the single-photon coupling efficiency.

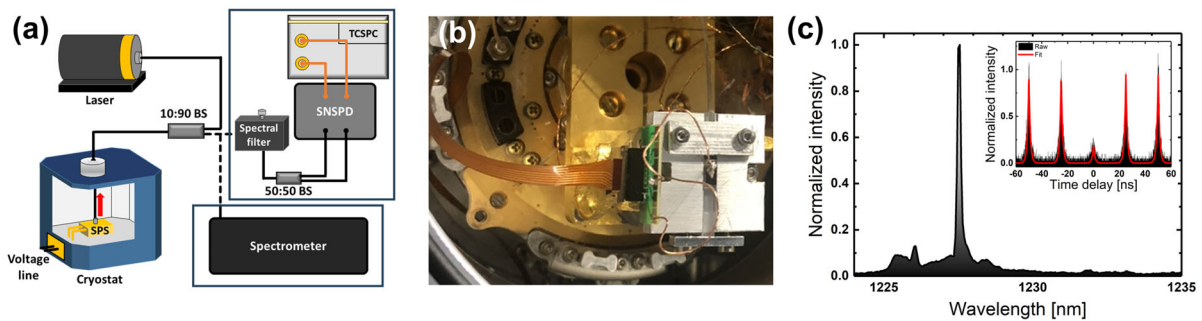


Figure 3. (a) Schematic of the all-fiber-connectorized optical setup for single-photon characterization. (b) Photo image of a multi-channel single-photon array mounted on a cryostat sample holder. (c) PL spectrum of the fiber-integrated cavity-coupled QD. Inset: Measured second-order correlation function of a single QD emission through the fiber channel.

The important advantage of our device-to-fiber integration is that it enables the pre-characterization of several QD devices from their original wafer and the selective integration of specific devices with desired properties. This was impossible with previous chip-to-fiber integrations. However, to bring this advantage, the device properties should remain consistent during the integration process. In particular, simply transferring the QD devices onto a fiber facet with a refractive index of about 1.45 results in a spectral shift of the cavity mode. To prevent this change, we etched the fiber core a 70 nm during the metal hole etching process, allowing the cavity to remain air-suspended even after fiber integration. Additionally, the interconnected design of hole-CBGs offers more robustness against potential deformation by the heterogeneous integration compared to conventional ring-CBGs. Therefore, our approach could enable pre-characterization and selective integration of multiple QD devices. To demonstrate this capability, we compared the PL spectrum of the QD device before and after the fiber integration. The comparison spectra in Figure 4(a) show that the pick-and-place integration with air-suspended integration preserves the cavity mode and QD frequency well before and after the transfer process. We attribute the small frequency shift of the QD peak to the small amount of induced tensile strain. From this feature, we carefully find the second QD device at a similar emission frequency and compare the spectrum before and after integration (Figure 4(b)). Two fiber-integrated QD devices display nearly identical emission frequencies, ensuring their similarity after fiber integration. This aspect holds significant importance in achieving multiple, identical quantum emitters with high yield and establishing scalable quantum interference or entanglement. Each QD device showed a measured fiber-coupling efficiency of 7% and 6%, respectively. The reason for lower coupling efficiency in experiments than the simulated value would be the unoptimized distance of a reflector and the uncontrolled position of QDs to the cavity center. This could be improved by introducing

site-controlled QD growth²⁸ or cavity fabrication^{3, 29} techniques. Furthermore, optimizing the etching depth of the fiber could increase the coupling efficiency further.³⁰

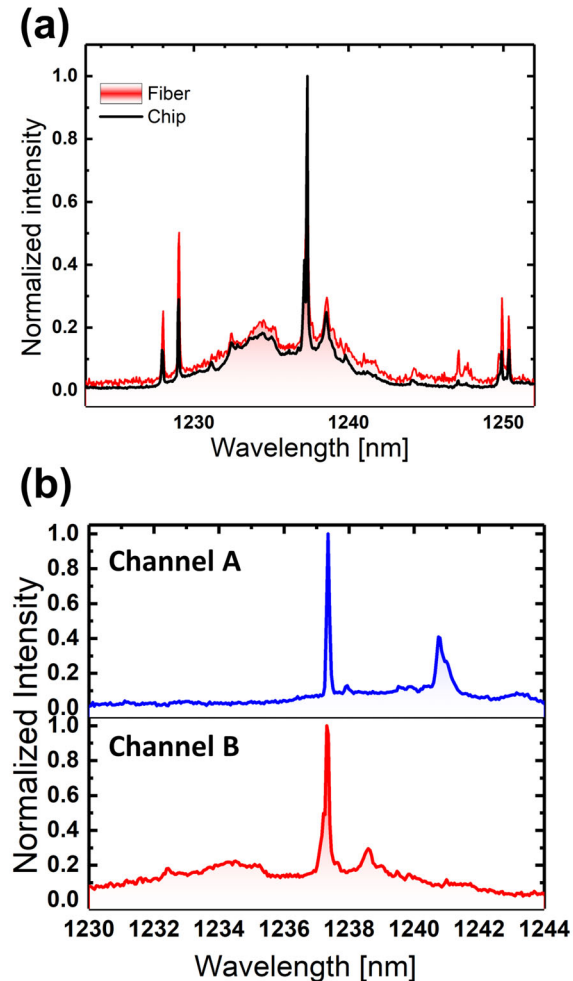


Figure 4. (a) Comparison of PL spectrum of the same QD device characterized before and after fiber integration. (b) PL spectra from two different QD devices integrated on different fiber channels.

We finally demonstrate a fine frequency tuning capability in the fiber-integrated platform. Although pre-characterization and selective integration secure multiple quantum channels with target frequencies, frequency tunability will be desired to eliminate any remaining detuning from the target frequency. To accomplish frequency tunability on fiber-integrated, we apply an electric field through the fiber-integrated electrodes on the front and back of QD devices. We estimate the distance between two electrodes to be about $7.7\text{ }\mu\text{m}$, calculated from the interference pattern in the PL spectrum. Increasing the applied voltage shifts the frequency of the QD device, as shown in Figure 5. At a voltage of 160 V, an electric field of up to 207.8 kV/cm is applied to the device. The result shows a possible tunability of the single-photon emission on the fiber-integrated platform, but the amount of shifts is relatively small. In this work, the distance between two electrodes was manually controlled using screws, but it could be controlled more precisely by mounting them in a piezo stage. Reducing the distance below $1\text{ }\mu\text{m}$ would be advantageous for increasing the applied field and fiber-coupling efficiency. Furthermore, implementing a p-i-n structure to the QD could extend a tuning range and also enable current operation, eliminating the laser excitation source.³¹

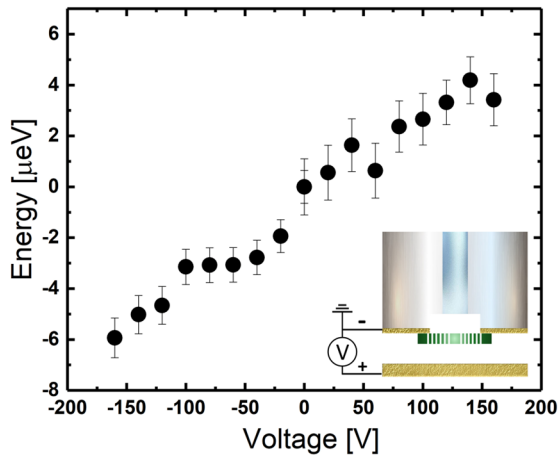


Figure 5. Frequency tuning of a single QD emission by fiber-integrated electrodes. The inset shows the configuration of voltage application system.

We have demonstrated fiber-integrated multi-channel, tunable single-photon sources. By combining an optimal nanophotonic cavity, device-to-fiber integration, and applying electric field techniques, the multi-functional fiber platform exhibits capabilities of low-temperature cooling, efficient single-photon transmission, selective integration, and frequency tunability, thereby enhancing the overall performance and adaptability of our fiber-integrated quantum photonic devices. This fiber-integrated platform directly interfaces all optical and electrical signals, eliminating the need for additional alignment processes. This offers a scalable and reliable quantum photonic resource for advanced applications. In particular, together with the matured fiber optics technologies and fiber-coupled multi-channel single-photon detectors, the development of fiber-integrated multi-channel quantum light sources can establish all-fiber-connected real-world quantum communications.^{14, 32, 33}

Corresponding Author

Je-Hyung Kim – Department of Physics, Ulsan National Institute of Science and Technology,
Ulsan 44919, Republic of Korea; Email: jehyungkim@unist.ac.kr

Author Contributions

The manuscript was written through the contributions of all authors. All authors have given approval to the final version of the manuscript.

Notes

Any additional relevant notes should be placed here.

ACKNOWLEDGMENT

This work is supported by the National Research Foundation of Korea (RS-2024-00438839, 2022R1A2C2003176), IITP (IITP-2024-2020-0-01606, RS-2023-00259676, RS-2023-00227854). M. Benyoucef acknowledges the support by the German Research Foundation - DFG (DeliCom, Heisenberg grant-BE 5778/4-1) and BMBF (QR.X). We thank R. Kaur, A. Kors for their assistance in the MBE growth process, J. P. Reithmaier for his discussion, and Dirk Albert for his technical assistance. The authors would like also to thank Prof. Edo Waks from the University of Maryland and C. J. K. Richardson from the Laboratory for Physical Sciences, University of Maryland, for the fruitful discussion and for providing initial testing QD samples.

REFERENCES

(1) Senellart, P.; Solomon, G.; White, A. High-performance semiconductor quantum-dot single-photon sources. *Nat. Nanotechnol.* **2017**, 12 (11), 1026-1039.

(2) Wang, H.; Hu, H.; Chung, T. H.; Qin, J.; Yang, X.; Li, J. P.; Liu, R. Z.; Zhong, H. S.; He, Y. M.; Ding, X.; Deng, Y. H.; Dai, Q.; Huo, Y. H.; Höfling, S.; Lu, C.-Y.; Pan, J.-W. On-Demand Semiconductor Source of Entangled Photons Which Simultaneously Has High Fidelity, Efficiency, and Indistinguishability. *Phys. Rev. Lett.* **2019**, 122 (11), 113602.

(3) Liu, J.; Su, R.; Wei, Y.; Yao, B.; Silva, S. F. C. d.; Yu, Y.; Iles-Smith, J.; Srinivasan, K.; Rastelli, A.; Li, J.; Wang, X. A solid-state source of strongly entangled photon pairs with high brightness and indistinguishability. *Nat. Nanotechnol.* **2019**, 14 (6), 586-593.

(4) Bremer, L.; Rodt, S.; Reitzenstein, S. Fiber-coupled quantum light sources based on solid-state quantum emitters. *Materials for Quantum Technology* **2022**, 2 (4), 042002.

(5) Muller, A.; Flagg, E. B.; Metcalfe, M.; Lawall, J.; Solomon, G. S. Coupling an epitaxial quantum dot to a fiber-based external-mirror microcavity. *Appl. Phys. Lett.* **2009**, 95 (17).

(6) Sartison, M.; Weber, K.; Thiele, S.; Bremer, L.; Fischbach, S.; Herzog, T.; Kolatschek, S.; Reitzenstein, S.; Herkommer, A.; Michler, P. 3d printed micro-optics for quantum technology: Optimized coupling of single quantum dot emission into a single mode fiber. *Light adv. manuf.* **2021**, 2, 6 (2021)

(7) Daveau, R. S.; Balram, K. C.; Pregnolato, T.; Liu, J.; Lee, E. H.; Song, J. D.; Verma, V.; Mirin, R.; Nam, S. W.; Midolo, L.; Stobbe, S.; Srinivasan, K.; Lodahl, P. Efficient fiber-coupled single-photon source based on quantum dots in a photonic-crystal waveguide. *Optica* **2017**, 4 (2), 178-184.

(8) Lee, C.-M.; Buyukkaya, M. A.; Aghaeimeibodi, S.; Karasahin, A.; Richardson, C. J. K.; Waks, E. A fiber-integrated nanobeam single photon source emitting at telecom wavelengths. *Appl. Phys. Lett.* **2019**, 114 (17), 171101.

(9) Ma, B.; Chen, Z.-S.; Wei, S.-H.; Shang, X.-J.; Ni, H.-Q.; Niu, Z.-C. Single photon extraction from self-assembled quantum dots via stable fiber array coupling. *Appl. Phys. Lett.* **2017**, 110 (14).

(10) Musiał, A.; Żołnacz, K.; Srocka, N.; Kravets, O.; Große, J.; Olszewski, J.; Poturaj, K.; Wójcik, G.; Mergo, P.; Dybka, K.; Dyrkacz, M.; Dłubek, M.; Lauritsen, K.; Bülter, A.; Schneider, P.-I.; Zschiedrich, L.; Burger, S.; Rodt, S.; Urbańczyk, W.; Sęk, G.; Reitzenstein, S. Plug&Play Fiber-Coupled 73 kHz Single-Photon Source Operating in the Telecom O-Band. *Adv. Quantum. Technol.* **2020**, 3 (6), 2000018.

(11) Żołnacz, K.; Musiał, A.; Srocka, N.; Große, J.; Schlösinger, M. J.; Schneider, P.-I.; Kravets, O.; Mikulicz, M.; Olszewski, J.; Poturaj, K.; Wójcik, G.; Mergo, P.; Dybka, K.; Dyrkacz, M.; Dłubek, M.; Rodt, S.; Burger, S.; Zschiedrich, L.; Sęk, G.; Reitzenstein, S.; Urbańczyk, W. Method for direct coupling of a semiconductor quantum dot to an optical fiber for single-photon source applications. *Opt. Express* **2019**, 27 (19), 26772-26785.

(12) Cadeddu, D.; Teissier, J.; Braakman, F. R.; Gregersen, N.; Stepanov, P.; Gérard, J.-M.; Claudon, J.; Warburton, R. J.; Poggio, M.; Munsch, M. A fiber-coupled quantum-dot on a photonic tip. *Appl. Phys. Lett.* **2016**, 108 (1).

(13) Jeon, W. B.; Moon, J. S.; Kim, K.-Y.; Ko, Y.-H.; Richardson, C. J. K.; Waks, E.; Kim, J.-H. Plug-and-Play Single-Photon Devices with Efficient Fiber-Quantum Dot Interface. *Adv. Quantum. Technol.* **2022**, 5 (10), 2200022.

(14) Takemoto, K.; Nambu, Y.; Miyazawa, T.; Sakuma, Y.; Yamamoto, T.; Yorozu, S.; Arakawa, Y. Quantum key distribution over 120 km using ultrahigh purity single-photon source and superconducting single-photon detectors. *Sci. Rep.* **2015**, *5* (1), 14383.

(15) Steinbrecher, G. R.; Olson, J. P.; Englund, D.; Carolan, J. Quantum optical neural networks. *npj Quantum Information* **2019**, *5* (1), 60.

(16) Wang, H.; He, Y.; Li, Y.-H.; Su, Z.-E.; Li, B.; Huang, H.-L.; Ding, X.; Chen, M.-C.; Liu, C.; Qin, J.; Li, J.-P.; He, Y.-M.; Schneider, C.; Kamp, M.; Peng, C.-Z.; Höfling, S.; Lu, C.-Y.; Pan, J.-W. High-efficiency multiphoton boson sampling. *Nat. Photonics* **2017**, *11* (6), 361-365.

(17) Uppu, R.; Midolo, L.; Zhou, X.; Carolan, J.; Lodahl, P. Quantum-dot-based deterministic photon–emitter interfaces for scalable photonic quantum technology. *Nat. Nanotechnol.* **2021**, *16* (12), 1308-1317.

(18) Li, J.-P.; Qin, J.; Chen, A.; Duan, Z.-C.; Yu, Y.; Huo, Y.; Höfling, S.; Lu, C.-Y.; Chen, K.; Pan, J.-W. Multiphoton Graph States from a Solid-State Single-Photon Source. *ACS Photonics* **2020**, *7* (7), 1603-1610.

(19) De Gregorio, M.; Yu, S.; Witt, D.; Lin, B.; Mitchell, M.; Dusanowski, Ł.; Schneider, C.; Chrostowski, L.; Huber-Loyola, T.; Höfling, S. Plug-and-Play Fiber-Coupled Quantum Dot Single-Photon Source via Photonic Wire Bonding. *Adv. Quantum. Technol.* **2024**, *7* (1), 2300227.

(20) Kors, A.; Reithmaier, J. P.; Benyoucef, M. Telecom wavelength single quantum dots with very small excitonic fine-structure splitting. *Appl. Phys. Lett.* **2018**, *112* (17).

(21) Kors, A.; Fuchs, K.; Yacob, M.; Reithmaier, J. P.; Benyoucef, M. Telecom wavelength emitting single quantum dots coupled to InP-based photonic crystal microcavities. *Appl. Phys. Lett.* **2017**, 110 (3).

(22) Li, L.; Chen, E. H.; Zheng, J.; Mouradian, S. L.; Dolde, F.; Schröder, T.; Karaveli, S.; Markham, M. L.; Twitchen, D. J.; Englund, D. Efficient Photon Collection from a Nitrogen Vacancy Center in a Circular Bullseye Grating. *Nano Lett.* **2015**, 15 (3), 1493-1497.

(23) Davanço, M.; Rakher, M. T.; Schuh, D.; Badolato, A.; Srinivasan, K. A circular dielectric grating for vertical extraction of single quantum dot emission. *Appl. Phys. Lett.* **2011**, 99 (4), 041102.

(24) Rickert, L.; Kupko, T.; Rodt, S.; Reitzenstein, S.; Heindel, T. Optimized designs for telecom-wavelength quantum light sources based on hybrid circular Bragg gratings. *Opt. Express* **2019**, 27 (25), 36824-36837.

(25) Liu, R.; Li, F.; Padgett, M.; Phillips, D. Generalized photon sieves: fine control of complex fields with simple pinhole arrays. *Optica* **2015**, 2 (12), 1028-1036.

(26) Kipp, L.; Skibowski, M.; Johnson, R. L.; Berndt, R.; Adelung, R.; Harm, S.; Seemann, R. Sharper images by focusing soft X-rays with photon sieves. *Nature* **2001**, 414 (6860), 184-188.

(27) Ates, S.; Sapienza, L.; Davanco, M.; Badolato, A.; Srinivasan, K. Bright Single-Photon Emission From a Quantum Dot in a Circular Bragg Grating Microcavity. *IEEE J. Sel. Top Quantum Electron.* **2012**, 18 (6), 1711-1721.

(28) Zhang, J.; Chattaraj, S.; Huang, Q.; Jordao, L.; Lu, S.; Madhukar, A. On-chip scalable highly pure and indistinguishable single-photon sources in ordered arrays: path to quantum optical circuits. *Sci. Adv.* **2022**, 8 (35), eabn9252.

(29) Liu, S.; Wei, Y.; Su, R.; Su, R.; Ma, B.; Chen, Z.; Ni, H.; Niu, Z.; Yu, Y.; Wei, Y. A deterministic quantum dot micropillar single photon source with > 65% extraction efficiency based on fluorescence imaging method. *Sci. Rep.* **2017**, 7 (1), 13986.

(30) Ma, C.; Yang, J.; Li, P.; Rugeramigabo, E. P.; Zopf, M.; Ding, F. Circular photonic crystal grating design for charge-tunable quantum light sources in the telecom C-band. *Opt. Express* **2024**, 32 (8), 14789-14800.

(31) Bennett, A. J.; Patel, R. B.; Skiba-Szymanska, J.; Nicoll, C. A.; Farrer, I.; Ritchie, D. A.; Shields, A. J. Giant Stark effect in the emission of single semiconductor quantum dots. *Appl. Phys. Lett.* **2010**, 97 (3), 031104.

(32) You, X.; Zheng, M.-Y.; Chen, S.; Liu, R.-Z.; Qin, J.; Xu, M.-C.; Ge, Z.-X.; Chung, T.-H.; Qiao, Y.-K.; Jiang, Y.-F. Quantum interference with independent single-photon sources over 300 km fiber. *Advanced Photonics* **2022**, 4 (6), 066003-066003.

(33) Reindl, M.; Huber, D.; Schimpf, C.; da Silva, S. F. C.; Rota, M. B.; Huang, H.; Zwiller, V.; Jöns, K. D.; Rastelli, A.; Trotta, R. All-photonic quantum teleportation using on-demand solid-state quantum emitters. *Sci. Adv.* **2018**, 4 (12), eaau1255.